Supporting Information

Ultrathin $MoSe_2$ Nanosheets Decorated on Carbon Fiber Cloth as Binder-Free and High-Performance Electrocatalyst for Hydrogen Evolution

Bin Qu, [†, ‡] *Xianbo Yu,* [†] *Yujin Chen,* [*,†] *Chunling Zhu,* [*,§] *Chunyan Li,*[*,†] *Zhuoxun Yin* [†] and *Xitian Zhang*[#]

† Key Laboratory of In-Fiber Integrated Optics, Ministry of Education, and College of Science, Harbin Engineering University , Harbin 150001, China

‡ Department of Applied Chemistry, College of Science, Northeast Agricultural University, Harbin 150030, China

§ College of Material Science and Chemical Engineering, Harbin Engineering University, Harbin 150001, China

Key Laboratory for Photonic and Electronic Bandgap Materials, Ministry of Education, and School of Physics and Electronic Engineering, Harbin Normal University, Harbin 150025, China.

*Corresponding authors. E-mail addresses: chenyujin@hrbeu.edu.cn, zhuchunling@hrbeu.edu.cn and chunyanli@hrbeu.edu.cn

Experimental Details: Pg S-3

Table S1: Comparison of HER performance among different $MoSe_2$ -based catalysts S-5

Table S2: Comparison of R_{ct} among different $MoSe_2$ -based catalysts. S-5

Table S3: Comparison of R_s among different $MoSe_2$ -based catalysts. S-5

Figure S1: HRTEM images showing pits highlighted by oval lines S-5

Figure S2: Structural characterizations of $MoSe_2$ spheres obtained at different reaction times at the presence of NH_4F in the reaction system, in which the carbon fiber cloth was not added. S-6

Figure S3: TEM image of solid $MoSe_2$ spheres obtained without NH_4F in the reaction system S-7

Figure S4: Raman spectra of our $MoSe_2$ catalysts S-7

Figure S5: Mo 3d and Se 3d XPS spectra of CMSF-6 a), CMSF-12 b) and CMS-9 c) S-8

Figure S6: Exchange current densities for all $MoSe_2$-based catalysts extracted from Tafel plots. S-9

Figure S7: Cyclic voltammograms in the region of 0.1–0.2 V vs. RHE for a) CMSF-6, b) CMSF-9, c) CMSF-12, d) CMS-9 and e) The differences in current density ($\Delta J = J_a - J_c$) at 0.15 V vs. RHE plotted against scan rate fitted to a linear regression allows for the estimation of C_{dl}. S-10

Figure S8: Cyclic voltammograms in the region of -0.2–0.6 V vs. RHE for CMSF-6, CMSF-9, CMSF-12 and CMS-9 S-11

Figure S9: Nyquist plots for a) CMSF-6, b) CMSF-9, c) CMSF-12 and d) CMS-9 at different overpotentials. S-11

Experimental details

Synthesis of catalysts. 30 mg of selenium powder was disolved in 5 mL hydrazine hydrate solution, and then 30 mg of MoO_3 powder, 400 mg of NH_4F, 10 mL distilled water and 15 mL ethanol were added under stirring. Carbon fiber cloth (area: 5 cm^2) was immersed into the solution above under ultrasonication for 10 min., and then the mixture was transferred to a Teflon-lined stainless steel autoclave with a capacity of 40 mL for solvent-thermal treatment at 220°C temperature for 6, 9, and 12 h, respectively. The autoclave was cooled down to room temperature naturally, and then the CMSFs were washed in distilled water and absolute ethanol under ultrasonication for 10 min, respectively, and dried in a vacuum oven at 60°C. The corresponding samples are named as CMSF-6, CMSF-9, and CMSF-12, respectively. For comparison, the additional sample was also prepared under the same conditions as those of CMSF-9, but NH_4F was not added into the reaction system. The sample was named as CMS-9.

Structural Characterization. The morphology and size of the samples were characterized by scanning electron microscope (HSD/SU70) and a FEI Tecnai-F20 transmission electron microscope equipped with a Gatan imaging filter (GIF). XPS measurements were carried out by using a spectrometer with Mg Kα radiation (PHI 5700 ESCA System). The binding energy was calibrated with the C 1s position of contaminant carbon in the vacuum chamber of the XPS instrument (284.6 eV). Raman spectroscopy was performed on the Raman microscope (JY-HR800, $\lambda_{excited}$ = 532nm).

Electrochemical measurements. Electrochemical measurements were performed in a three-electrode system at an electrochemical station (CHI660D). The three-electrode configuration was adopted for polarization and electrolysis measurements, where an Ag/AgCl (KCl saturated) electrode, a graphite rod and $MoSe_2$-based catalysts were used as the reference electrode, the counter electrode and the working electrode respectively. Linear sweep voltammetry with scan rate of 3 mV s^{-1} was conducted in 0.5 M H_2SO_4. For a Tafel plot, the linear portion is fit to the Tafel equation. All data has been corrected for a small ohmic drop based on impedance spectroscopy. All the potentials were calibrated to a reversible hydrogen electrode (RHE).

Table S1. Comparison of HER performance among different $MoSe_2$-based catalysts

Catalyst type	Tafel slope [mV dec^{-1}]	Exchange current j_0 [μA cm^{-2}]	Onset η [mV]	η [mV] at j_{10}	Refs
$MoSe_2$ thin film	105-120	2.0	200	—	18
$MoSe_2$ thin film	59.8	0.38	—	250	19
$MoSe_2$ nanosheets	101	—	150	290	21
$MoSe_2$/RGO hybrid	69	—	50	115	21
$MoSe_2$ nanosheets	106	—	150-260	—	12
S-doped $MoSe_2$	60	—	90	—	12
$MoSe_{2-x}$ nanosheets	98	—	170	288	13
CMSF-6	69	6.0	145	222	This work
CMSF-9	69	21.1	70	182	This work
CMSF-12	73	23.3	97	198	This work
CMS-9	76	14.4	115	206	This work

Table S2. Comparison of R_{ct} among different $MoSe_2$-based catalysts. Unit: Ω cm^{-2}

Catalysts	R_{ct} at 300 mV	R_{ct} at 250 mV	R_{ct} at 200 mV	R_{ct} at 150 mV
CMSF-6	3.2	9.1	133.2	380
CMSF-9	0.7	1.0	6.5	116.8
CMSF-12	0.8	1.9	7.9	244.5
CMS-9	2.0	4.9	24.4	316.5

Table S3. Comparison of R_s among different $MoSe_2$-based catalysts. Unit: Ω cm^{-2}

Catalysts	R_s
CMSF-6	1.5
CMSF-9	1.4
CMSF-12	1.6
CMS-9	1.7

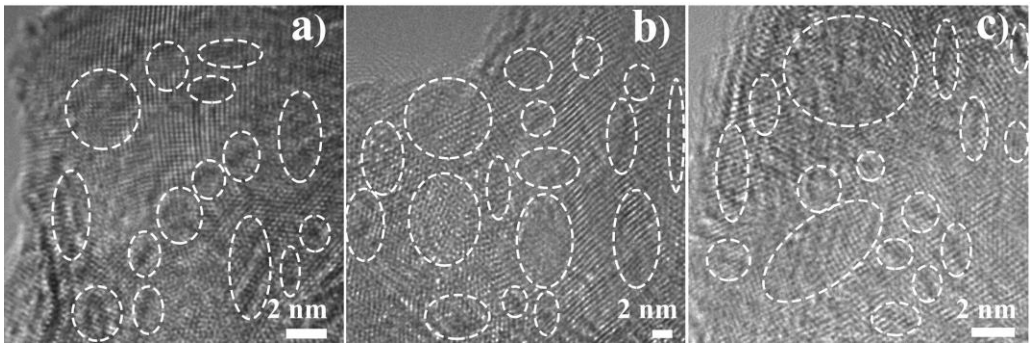

Figure S1 HRTEM images of CMSF-6, CMSF-9 and CMSF-12 showing pits highlighted by oval lines

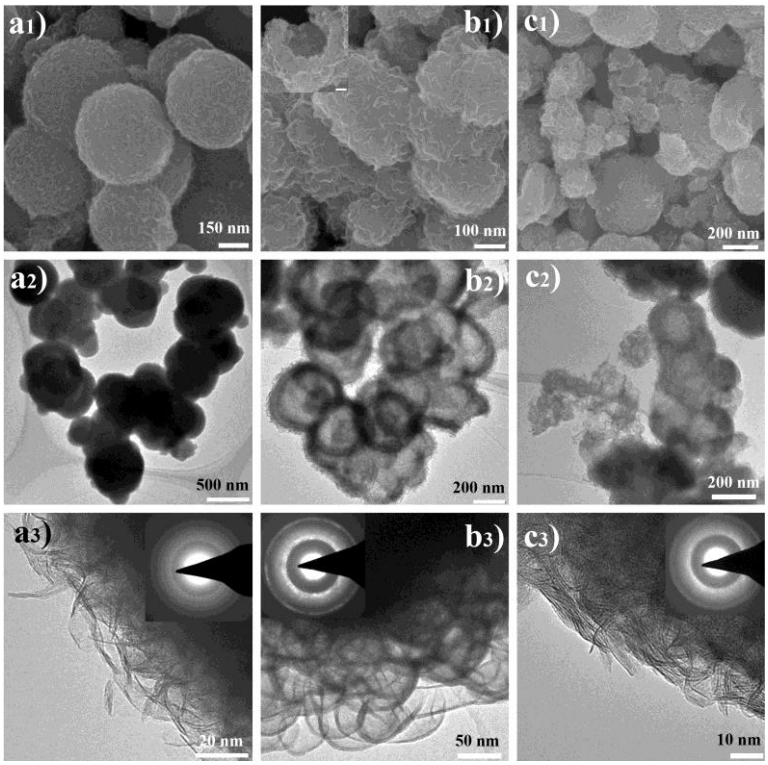

Figure S2 Structural characterizations of $MoSe_2$ spheres obtained at different reaction times at the presence of NH_4F in the reaction system, in which the carbon fiber cloth was not added. a) $MoSe_2$ spheres obtained at a reaction time of 6 h, a_1) SEM image, and a_2-a_3) TEM images. The inset in a_3) showing the SAED pattern. b) $MoSe_2$ spheres obtained at a reaction time of 9 h, a_1) SEM image, and b_2-b_3) TEM images. The inset in b_1) showing a broken $MoSe_2$ sphere, scale bar: 100 nm and the inset in b_3) showing the SAED pattern. c) $MoSe_2$ spheres obtained at a reaction time of 12 h, c_1) SEM image, and c_2-c_3) TEM images. The inset in c_3) showing the SAED pattern.

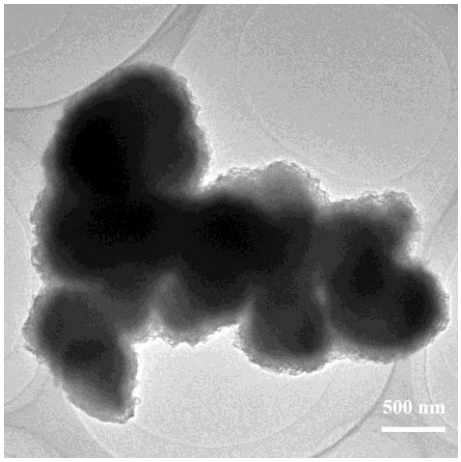

Figure S3 TEM image of solid $MoSe_2$ spheres obtained without NH_4F in the reaction system

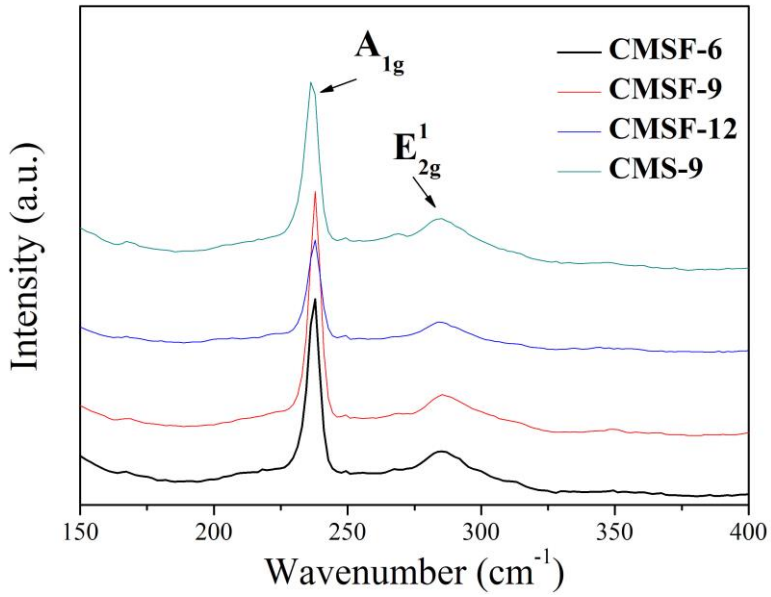

Figure S4 Raman spectra of CMSF-6,CMSF-9, CMSF-12 and CMS-9.

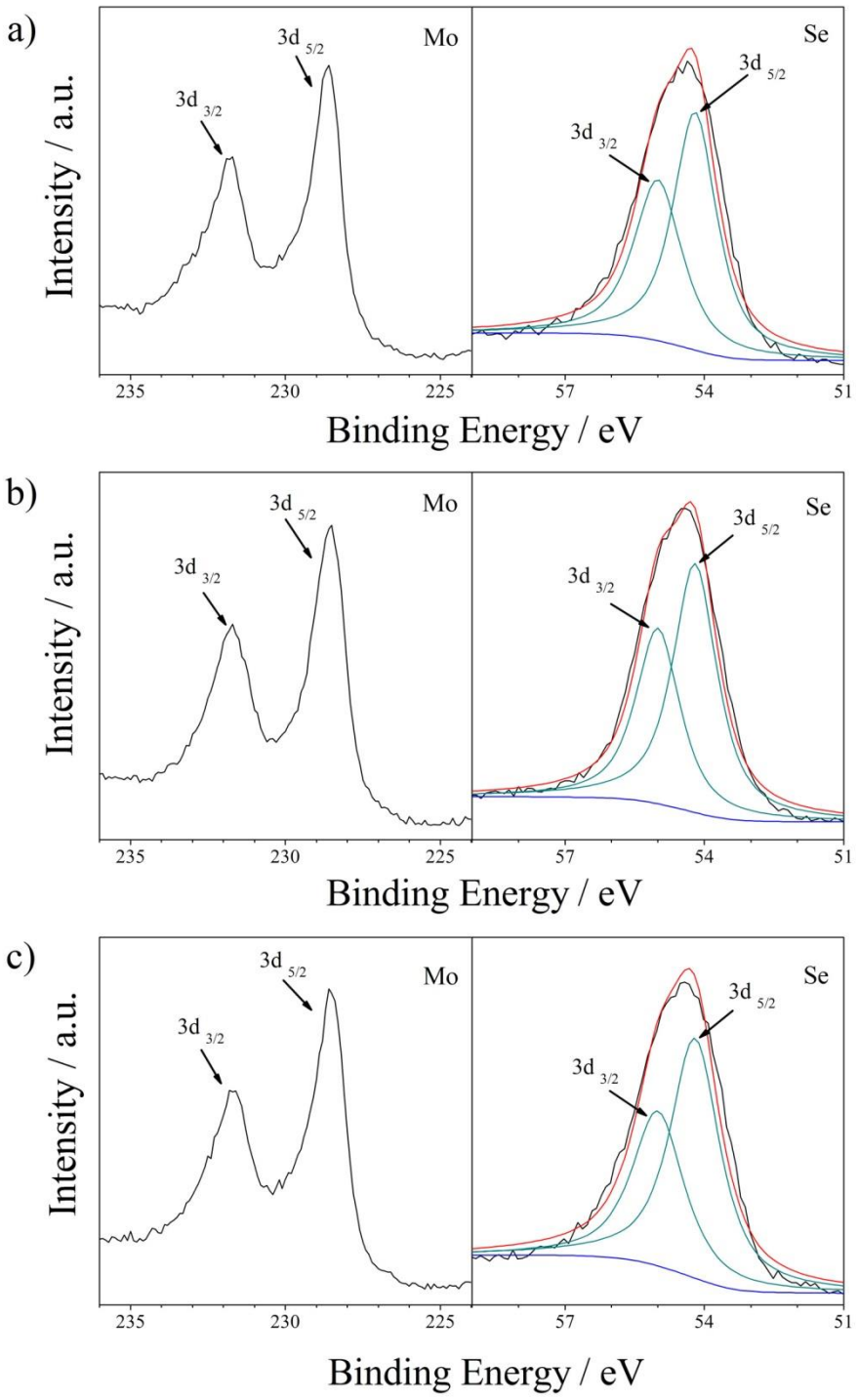

Figure S5 Mo 3d and Se 3d XPS spectra of CMSF-6 (a), CMSF-12 (b) and CMS-9 (c).

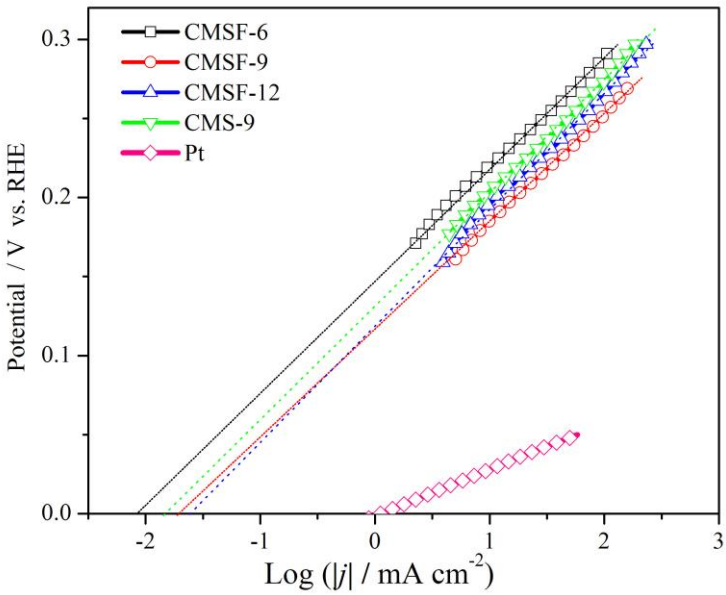

Figure S6 Exchange current densities for all $MoSe_2$-based catalysts extracted from Tafel plots.

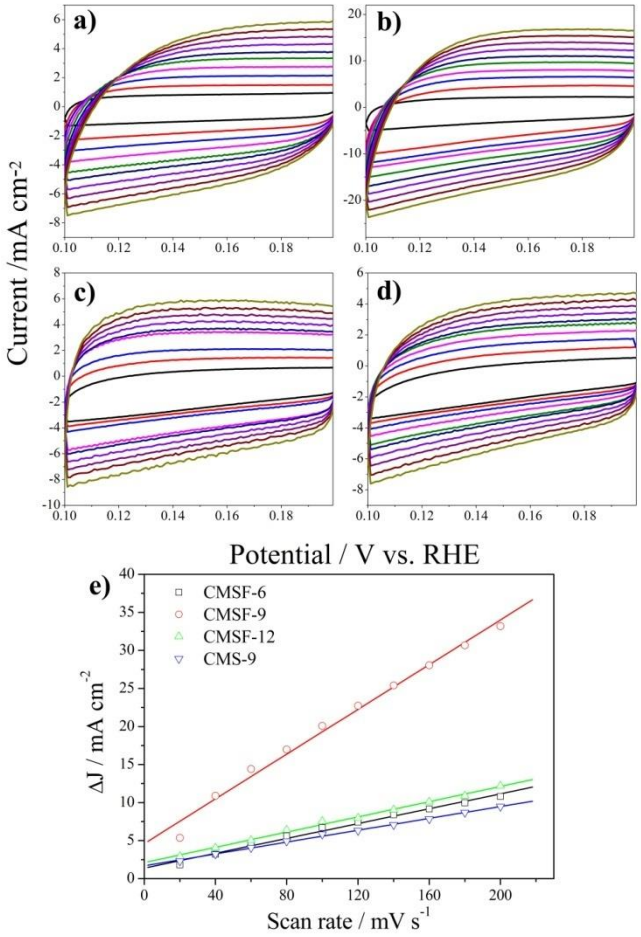

Figure S7 Cyclic voltammograms in the region of 0.1–0.2 V vs. RHE for a) CMSF-6, b) CMSF-9, c) CMSF-12 and d) CMS-9. e) The differences in current density ($\Delta J = J_a - J_c$) at 0.15 V vs. RHE plotted against scan rate fitted to a linear regression allows for the estimation of C_{dl}.

The estimation of the effective active surface area of the samples was carried out according to literature. Cyclic voltammetry (CV) were performed at various scan rates (20, 40, 60 mV s^{-1}, etc.) in 0.1–0.2 V vs. RHE region. The double-layer capacitance (C_{dl}) of various samples can be determined from the cyclic voltammograms, which is expected to be linearly proportional to the effective surface area (Figure S7 a-d). The exact determination of the surface area is difficult due to the unknown capacitive behavior of the $MoSe_2$ nanosheets, but we can safely estimate the relative surface areas. CV measurements were taking in the region of 0.1-0.2 V vs. RHE, which could be mostly considered as the double-layer capacitive behavior. The double-layer capacitance is estimated by plotting the ΔJ (Ja-Jc) at 0.15 V vs. RHE against the scan rate, where the slope is twice C_{dl} (Figure S7 e). The C_{dl} were calculated to be 24.4 mF, 73.5 mF, 25.0 mF and 19.5 mF for CMSF-6, CMSF-9, CMSF-12 and CMS-9, respectively.

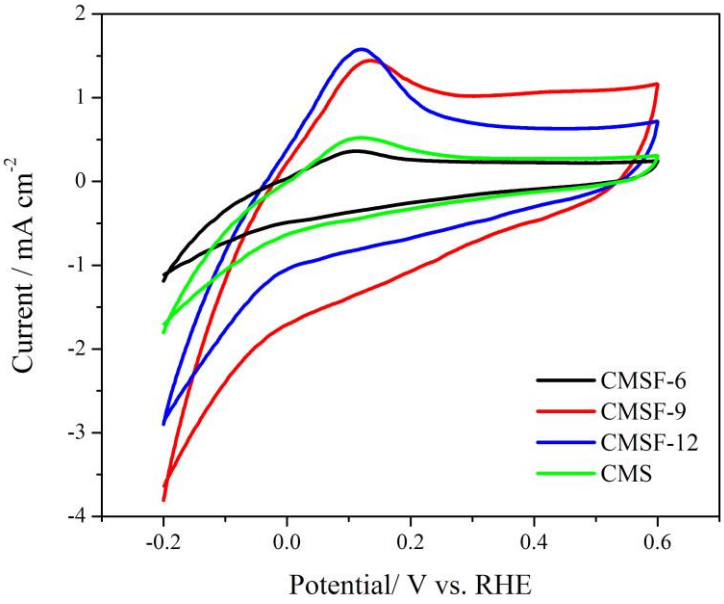

Figure S8 Cyclic voltammograms (CV) in the region of –0.2 to 0.6 V *vs.* RHE for our $MoSe_2$-based catalysts at pH=7.0. Scan rate: 50 mV s^{-1}.

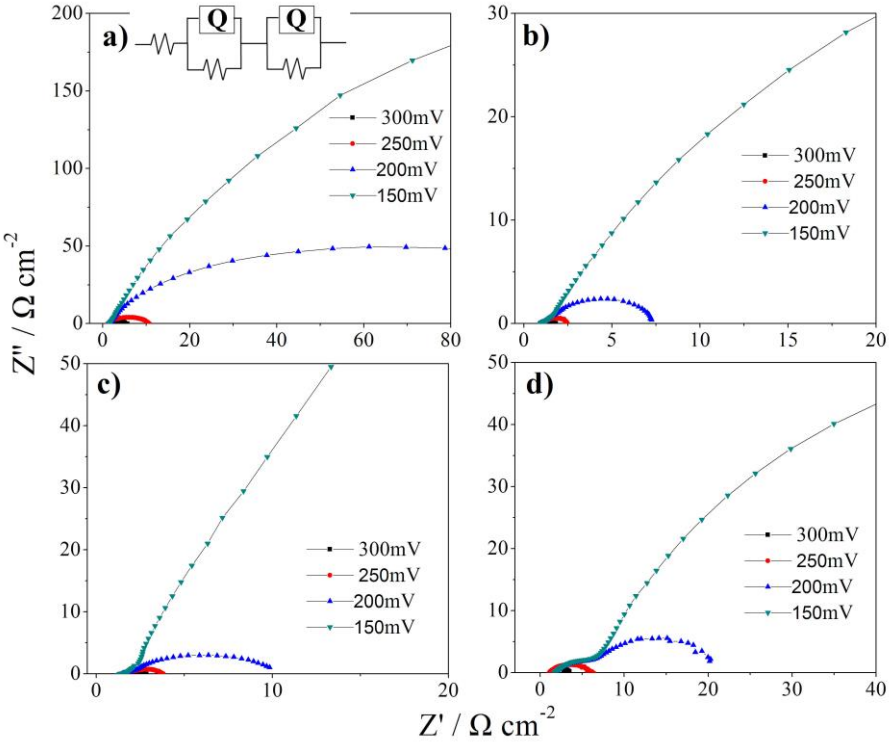

Figure S9 Nyquist plots for a) CMSF-6, b) CMSF-9, c) CMSF-12 and d) CMS-9 at different overpotentials.